helpful. We are then left with the familiar problem of full diagonalization of the Hamiltonian without knowledge of any basis functions that achieve partial blocking.

Summary

In this paper, we have investigated the detailed application of tensor surface harmonic theory to the structure and bonding of transition-metal clusters and related species. We have shown that a simple, unified treatment may be applied despite the large number of orbitals involved. The proposed scheme has firm group-theoretical foundations, and is shown to encapsulate the ideas of the isolobal principle. When combined with other TSH results, the theory can rationalize the electron counts of a diverse range of species, including metallaboranes and transition-metal clusters with a single main-group atom in the skeleton. We have also discussed the use of TSH theory to investigate the electron counts of very large metal clusters.

The main advantage of the method is that it enables generalized electron counting rules to be deduced from firm theoretical principles. Such derivations are particularly straightforward for closo deltahedra. More detailed treatments also enable us to rationalize the bonding in nido and arachno species and in large transition-metal cluster carbonyls with interstitial moieties. Such structure–electron count correlations are useful in making predictions about real chemical reactions.[20] For example, the disposition of the nonbonding orbital in polar clusters helps us to rationalize deviations from the usual electron-counting rules and predict reactivity.

Further applications to the theoretical study of fluxional processes in both main-group and transition-metal clusters[11] may be of great importance in future work. Recent developments include the development of a qualitative center-of-gravity rule for the splitting of cluster orbitals,[45] a tensor solid harmonic theory for multishell clusters, more detailed studies of cluster hybridization[21] and the pairing principle,[29] and the use of TSH theory in the interpretation of cluster NMR data.[46]

Acknowledgment. We wish to thank Dr. R. G. Woolley and Dr. D. M. P. Mingos for their useful comments on the manuscript, Dr. Catherine Housecroft for some helpful discussions, and the SERC for financial support.

(45) Wales, D. J.; Mingos, D. M. P. *Inorg. Chem.*, in press.
(46) Wales, D. J.; Mingos, D. M. P. Manuscript in preparation.

Contribution from the Departments of Chemistry, University of Denver, Denver, Colorado 80208, and University of Colorado at Denver, Denver, Colorado 80204

Metal-Nitroxyl Interactions. 54. EPR Spectra of High-Spin Iron(III) Complexes of Spin-Labeled Tetraphenylporphyrins in Frozen Solution

Lee Fielding, Kundalika M. More, Gareth R. Eaton,* and Sandra S. Eaton*

Received December 15, 1988

Frozen-solution EPR spectra were obtained for high-spin iron(III) complexes of seven ortho-spin-labeled tetraphenylporphyrins and four iron(III) porphyrin complexes with nitroxyl carboxylates as axial ligands. Data obtained at 5–12 K provided examples of iron–nitroxyl spin–spin interactions ranging from small perturbations of the iron and nitroxyl line widths to $|J| = 0.17$ cm^{-1}. Increasing iron relaxation rates at higher temperatures caused collapse of the spin–spin splittings due to interactions with $|J| < \sim 0.05$ cm^{-1}. Multiple conformations with different magnitudes of spin–spin interaction were observed for the complexes of the ortho-spin-labeled porphyrins. Six-coordination of the iron or π complexation of the porphyrin ring favored population of the conformations with weaker electron–electron spin–spin interaction. The stronger electron–electron spin–spin interactions are assigned to conformations with weak orbital overlap between the ortho substituent and orbitals of the porphyrin π system or the metal.

Introduction

Interpretations of EPR spectra obtained for biological samples including photosynthetic systems,[1,2] spin-labeled cytochrome P450,[3,4] and spin-labeled iron transferrin[5] have invoked electron–electron spin–spin interaction between organic radicals and paramagnetic iron centers.[6] Analysis of spectra of this type could be facilitated by comparison with data for small molecules that demonstrate the effects of interaction between paramagnetic iron(III) and organic radicals on the EPR spectra. Studies are therefore under way to characterize these effects.

A series of spin-labeled iron porphyrins (I–XI, Chart I) were selected to provide a range of strengths of the iron–nitroxyl spin–spin interaction. In I–VII the length of the ortho substituent between the porphyrin and the nitroxyl rings was varied. Frozen-solution EPR spectra of the low-spin iron(III) complexes $Fe(P)L_2$, P = I–VII, L = imidazole or 1-methyl-imidazole, provided examples of spectra due to exchange interaction up to 0.28 cm^{-1} and provided a basis for interpretation[7] of the previously reported spectra for spin-labeled cytochrome P450. The fluid-solution EPR spectra of high-spin VIII–XI and Fe(P)X, P = I–VII, X = F^-, Cl^-, Br^-, I^-, demonstrated that the nitroxyl signal broadened and shifted to higher g value as the strength of the iron–nitroxyl spin–spin interaction increased.[8] We now report EPR studies of high-spin VIII–XI and of the high-spin iron(III) complexes of spin-labeled porphyrins I–VII in frozen solution.

Experimental Section

Physical Measurements. X-Band EPR spectra were obtained on a Varian E9 spectrometer interfaced to a Varian 620/L103 or IBM C-S9000 laboratory computer or on an IBM ER200 spectrometer interfaced to an IBM CS9000 computer. The lines in most of the EPR spectra were sufficiently broad that the spectra were unchanged by degassing. Therefore, the spectra discussed below were obtained on air-saturated samples unless otherwise noted. Sample concentrations were about 1 mM except for experiments designed to check for concentration dependence. All spectra were obtained at microwave powers that did not cause saturation of the signal and with 100-kHz modulation at amplitudes that did not distort the line shapes. Quantitation of the nitroxyl EPR signals was done by comparison of the double integrals of the spectra with double integrals for solutions of known concentrations of 2,2,6,6-tetramethylpiperidin-1-yl or 4-oxo-2,2,6,6-tetramethylpiperidin-1-yl in the same

* To whom correspondence should be addressed: G.R.E., University of Denver; S.S.E., University of Colorado at Denver.

(1) Ito, S.; Tang, X. S.; Sato, K. *FEBS Lett.* **1986**, *205*, 275.
(2) Beijer, C.; Rutherford, A. W. *Biochim. Biophys. Acta* **1987**, *890*, 169.
(3) Pirrwitz, J.; Lassman, G.; Rein, H.; Ristau, O.; Janig, G. R.; Ruckpaul, K. *FEBS Lett.* **1977**, *83*, 15.
(4) Pirrwitz, J.; Lassman, G.; Rein, H.; Janig, G. R.; Pecar, S.; Ruckpaul, K. *Acta Biol. Med. Ger.* **1979**, *38*, 235.
(5) Najarian, R. C.; Harris, D. C.; Aisen, P. *J. Biol. Chem.* **1978**, *253*, 38.
(6) Eaton, S. S.; Eaton, G. R. *Biol. Magn. Reson.*, in press.
(7) Fielding, L.; More, K. M.; Eaton, G. R.; Eaton, S. S. *J. Am. Chem. Soc.* **1986**, *108*, 618.
(8) Fielding, L.; More, K. M.; Eaton, G. R.; Eaton, S. S. *Inorg. Chem.* **1987**, *26*, 856.

0020-1669/89/1328-3127$01.50/0

Chart I

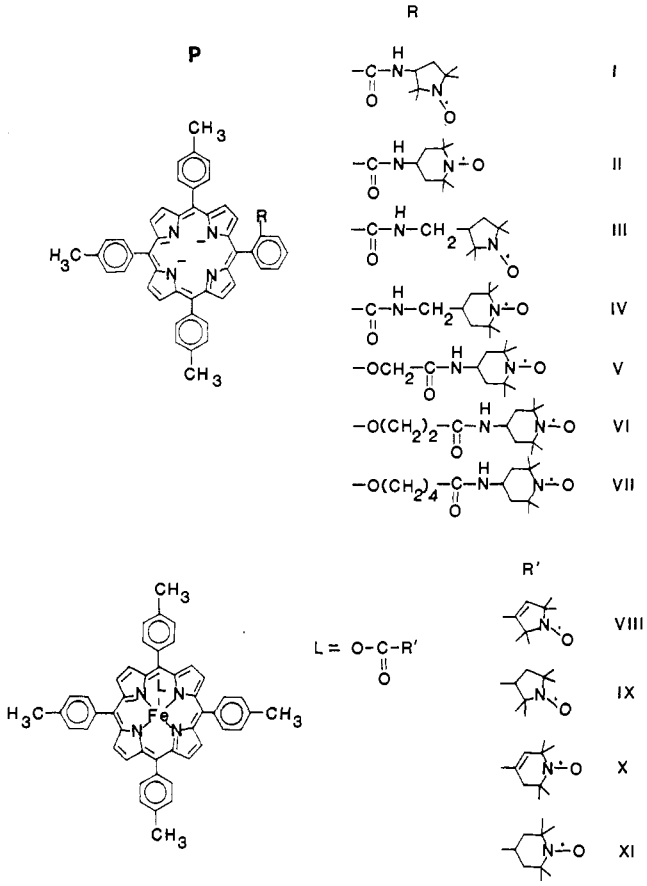

solvent and sample tube. Throughout the ensuing text, integration and integrals refer to double integrals of the first derivative spectra.

Preparation of Compounds. Spin-labeled iron porphyrins Fe(P)Cl (P = I–VII),[7] Fe(TTP)Cl,[9,10] and VIII–XI[8] were prepared as previously reported. Replacement of the axial anions of Fe(P)X, P = I–VIII, was performed by the same procedures as were used in the preparation of solutions for EPR studies in fluid solution.[8] 1,3,5-Trinitrobenzene was recrystallized from ethanol.

Computer Simulations. The frozen-solution EPR spectra were simulated with a program (METNO) that uses Belford's fourth-order frequency shift perturbation method.[11,12] The Hamiltonian included the Zeeman interactions for $S = {}^5/_2$ iron(III) and $S = {}^1/_2$ nitroxyl, the iron zero-field splitting, dipolar interaction between the two paramagnetic centers, and an isotropic exchange interaction. A negative sign of J indicates an antiferromagnetic interaction. The orientation of the interspin vector was defined by ϵ, the angle between the iron z axis and the interspin vector, and η, the angle between the iron y axis and the projection of the interspin vector on the iron xy plane. The nitroxyl nitrogen hyperfine coupling was not included in the program so calculations were limited to spectra in which the line widths of the nitroxyl signals were greater than the nitroxyl hyperfine splitting and values of J were much greater than the nitroxyl nitrogen hyperfine. The orientation of the axes for the anisotropic nitroxyl g values can be defined in the program, but the g anisotropy is so small that it had no observable impact on the spectra calculated in this study. The nitroxyl g values were $g_x = 2.0089$, $g_y = 2.0062$, and $g_z = 2.0027$.[13] The g values for $S = {}^5/_2$ iron were assumed to be about 2.0.[14-16] Literature values for the zero-field-splitting parameter (ZFS)

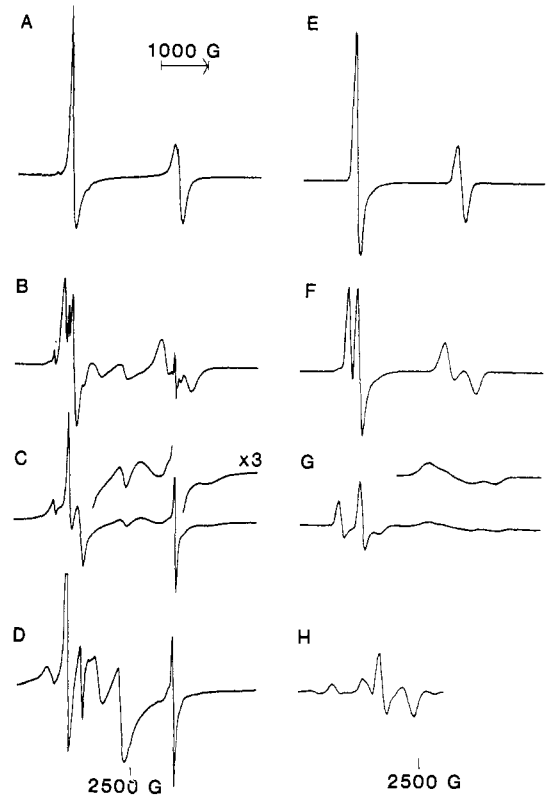

Figure 1. 5000-G scans of X-band (9.2 GHz) EPR spectra for spin-labeled iron(III) porphyrins in frozen toluene solution and computer simulations: (A) Fe(VII)F at 12 K; (B) Fe(V)Cl at 8 K; (C) Fe(III)F at 6 K; (D) Fe(I)Cl at 5 K. The spectra were obtained with microwave powers between 2 and 4 mW and modulation amplitudes of 1.25–2.0 G. The parameters used in the simulations were (E) $J = 0.0$ cm^{-1}, $r = 10$ Å, $\epsilon = 45°$, $\eta = 10°$, (F) $J = -0.015$ cm^{-1}, $r = 7.0$ Å, $\epsilon = 45°$, $\eta = 10°$, (G) $J = -0.032$ cm^{-1}, $r = 6.0$ Å, $\epsilon = 15°$, $\eta = 10°$, and (H) $J = -0.16$ cm^{-1}, $r = 7.0$ Å, $\epsilon = 65°$, $\eta = 35°$. Additional parameters are given in the text.

D are Fe(TPP)Cl, 6.0,[17] 6.5,[18] and 7.0 cm^{-1},[19] [Fe(TPP)(DMSO)$_2$]Cl, 10 cm^{-1},[20] and Fe(TPP)Br, 12.5 cm^{-1}.[21,22] It was assumed that the value of D for Fe(P)OH was similar to those reported for Fe(TPP)OMe, 3.0 cm^{-1},[19] and Fe(P)OH where P is a picket fence porphyrin, 5.3 cm^{-1}.[23] Since the value of D for Fe(protoporphyrin IX)F is 5.6 cm^{-1} [24] and ZFS values for iron tetraphenylporphyrins tend to be slightly smaller than for natural porphyrins,[17,19] the value of D for Fe(P)F was assumed to be between 3.0 and 5.0 cm^{-1}. Since the EPR spectra of Fe(TPP)X, X = F$^-$, Cl$^-$, and Br$^-$, show no rhombic splitting of $g_\perp$, it was assumed that the zero-field-splitting parameter E was 0. The value of E for Fe(P)OH was estimated to be about 0.1 cm^{-1}.[25] The simulations of the EPR spectra were insensitive to changes of ± 1 cm^{-1} in the value of D so the uncertainties in these parameters do not affect the interpretation of the EPR spectra of the spin-labeled complexes. The simulated spectra were sensitive to the sign of J. However, the changes in the spectra that occurred when the sign of J was changed could be compensated by changes in other parameters. Thus, the analysis of the spectra in this paper results in an ambiguity in the sign of J.

(9) Abbreviations: P, a porphyrin dianion; TPP, dianion of 5,10,15,20-tetraphenylporphyrin; TTP, dianion of 5,10,15,20-tetra(*p*-tolyl)-porphyrin; DMSO, dimethyl sulfoxide; TNB, 1,3,5-trinitrobenzene.

(10) Adler, A. D.; Longo, F. R.; Kampas, F.; Kim, J. *J. Inorg. Nucl. Chem.* **1970**, *32*, 2443.
(11) Belford, R. L.; Davis, P. H.; Belford, G. G.; Lenhardt, T. M. Extended Interactions Between Metal Complexes. *ACS Symp. Ser.* **1974**, No. 5, 40.
(12) Scullane, M. I.; White, L. K.; Chasteen, N. D. *J. Magn. Reson.* **1982**, *47*, 383.
(13) Eaton, S. S.; More, K. M.; Sawant, B. M.; Boymel, P. M.; Eaton, G. R. *J. Magn. Reson.* **1983**, *52*, 435.
(14) White, W. I. In *The Porphyrins*; Dolphin, D., Ed.; Academic Press: New York, 1978; Vol. V, p 303.
(15) Due to the large ZFS values for high-spin Fe(III) porphyrins, the EPR spectra are frequently described by a fictitious $S' = {}^1/_2$ with $g_\parallel = 2$ and $g_\perp = 6$.[16] This notation is also convenient for describing the experimental data. The turning points in the spectra correspond to an isotropic $g = 2$ when the true $S = {}^5/_2$ is used in the Hamiltonian.
(16) Wertz, J. E.; Bolton, J. R.; *Electron Spin Resonance*; McGraw-Hill: New York, 1972; pp 308–310, 386–388.
(17) Behere, D. V.; Mitra, S. *Inorg. Chem.* **1979**, *18*, 1723.
(18) Uenoyama, H. *Biochim. Biophys. Acta* **1971**, *230*, 479.
(19) Dolphin, D. H.; Sams, J. R.; Tsin, T. B.; Wong, K. L. *J. Am. Chem. Soc.* **1978**, *100*, 1711.
(20) Behere, D. V.; Birdy, R.; Mitra, S. *Inorg. Chem.* **1984**, *23*, 1978.
(21) Behere, D. V.; Date, S. K.; Mitra, S. *Chem. Phys. Lett.* **1979**, *68*, 544.
(22) Behere, D. V.; Birdy, R.; Mitra, S. *Inorg. Chem.* **1981**, *20*, 2786.
(23) Gunter, M. J.; Mclaughlin, G. M.; Berry, K. J.; Murray, K. S.; Irving, M.; Clark, P. E. *Inorg. Chem.* **1984**, *23*, 1984.
(24) Brackett, G. C.; Richards, P. L.; Caughey, W. S. *J. Chem. Phys.* **1971**, *54*, 4383.
(25) Fielding, L.; Eaton, G. R.; Eaton, S. S. *Inorg. Chem.* **1985**, *24*, 2309.

Results and Discussion

Iron(III) complexes of spin-labeled porphyrins I–VII were studied as the five-coordinate axial halides (Fe(P)X) and as the $(DMSO)_2$ adducts ($Fe(P)(DMSO)_2^+$). Four iron porphyrins, VIII–XI, with nitroxyl carboxylates as the axial ligand were also studied. Spectra obtained at 5–12 K that demonstrate the changes that occur for the iron and nitroxyl signals as the strength of the iron–nitroxyl interaction increases are shown in Figure 1.

The EPR spectrum of Fe(VII)F at 12 K had a broadened nitroxyl signal with a peak-to-peak line width of about 180 G and an iron signal at $g \sim 6$ (Figure 1A). These signals are attributed to weak electron–electron spin–spin interaction between the iron and nitroxyl centers. For Fe(VII)X, X = Cl^-, Br^-, and OH^-, at 5–12 K broadened nitroxyl signals with line widths of about 300 G were superimposed on sharper nitroxyl signals with partially resolved nitrogen hyperfine splittings, which indicates that the molecules exist in two conformations with differing strengths of the spin–spin interaction. In the ^1H NMR spectra of Fe(P)X, where P is analogous to VII but with the nitroxyl group replaced by a *tert*-butyl group and X = Cl^-, Br^-, and I^-, the signals for the *tert*-butyl group were at 5–12 ppm upfield of TMS with line widths of 25–50 Hz.[26] The impact of the iron on the *tert*-butyl signal implied that the side chain was located above the porphyrin plane rather than beside the plane. A similar conformation of the spin-labeled side chain could position the nitroxyl close enough to the iron to give iron–nitroxyl interaction despite the long through-bond pathway between the metal and the nitroxyl. This could occur via dipolar interaction or weak orbital overlap as discussed below.

The spectrum of Fe(V)Cl at 8 K (Figure 1B) has contributions from several conformations with varying strengths of spin–spin interaction. The sharp weak signals at $g \sim 6$ and $g \sim 2$ in Figure 1B–D are due to small amounts of conformations with negligible spin–spin interaction or to small amounts of decomposition products. The dominant species in Figure 1B exhibits a splitting of the iron $g \sim 6$ signal of about 170 G (1400 MHz) and a splitting of the nitroxyl signal of about 500 G (1400 MHz). Similar pairs of doublets were observed for Fe(V)X, X = F^- and Br^-.[27] The signals at $g \sim 9$, 4.7, and 3 are due to conformations with stronger spin–spin interaction, which are discussed below. The simulated spectrum in Figure 1F was obtained with $J = -0.015$ cm^{-1} and $r = 7.0$ Å. Similar calculated spectra resulted for $|J| = 0.013$–0.018 cm^{-1} and values of r between 6.0 and 8.0 Å for different orientations of the interspin vector relative to the iron axis system.

Multiple molecular conformations also contribute to the spectrum of Fe(III)F at 6 K (Figure 1C). The dominant species has broad nitroxyl and iron lines with splittings between the outermost components of about 1100 and 350 G (3000 MHz), respectively. The peaks at $g \sim 3$ and 9 are due to conformations with stronger spin–spin interaction. The spectrum in Figure 1G was calculated with $J = -0.032$ cm^{-1} and $r = 6$ Å. Comparable agreement between calculated and observed spectra was obtained for $|J|$ between 0.032 and 0.04 cm^{-1} and values of r between 6 and 8 Å.

In the spectrum of Fe(I)Cl at 5 K the dominant species has peaks that are shifted substantially from the g values for noninteracting iron or nitroxyl (Figure 1D). The simulated spectrum in Figure 1H was obtained with $J = -0.16$ cm^{-1} and $r = 7$ Å. The uncertainty in $|J|$ is about 0.01 cm^{-1}.

Since several conformations with differing magnitudes of the spin–spin interaction contribute to each of the spectra in Figure 1B–D, the changes in the spectra as a function of increasing interaction are more readily seen in the calculated spectra than in the experimental spectra. As the strength of the iron–nitroxyl interaction increases, the nitroxyl signal and the iron $g \sim 6$ signal appear to split into doublets. The splitting in energy units is equal for the two signals, but conversion from energy units into gauss

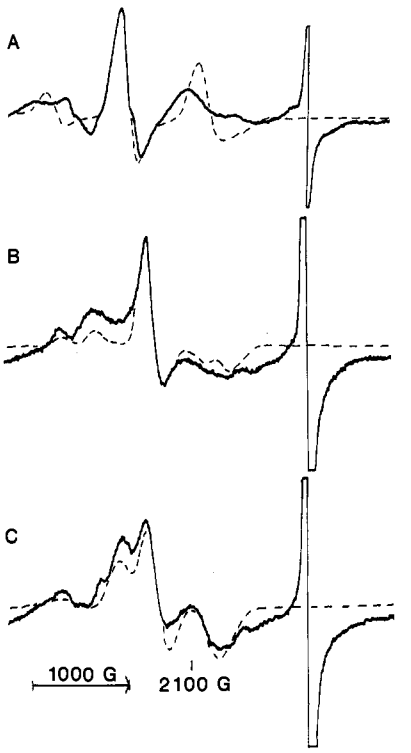

Figure 2. 4000-G scans of X-band (9.1 GHz) EPR spectra for Fe(I)X in toluene solution at 100 K: (A) X = F^-; (B) X = OH^-; (C) = Cl^-. The spectra were obtained with 10–20-G modulation amplitude and 50–100-mW microwave power. The $g \sim 6$ signal for weakly interacting iron was digitally subtracted to facilitate observation of the spectrum for the spin-coupled complex. The dotted lines represent simulated spectra obtained with the following parameters: (A) $J = 0.07$ cm^{-1}, $r = 7.0$ Å, $\epsilon = 35°$, $\eta = 35°$, $D = 3.0$ cm^{-1}, $E = 0.0$ cm^{-1}; (B) same as in part A except $J = 0.16$ cm^{-1}, $E = 0.10$ cm^{-1}; (C) same as in part A except $J = 0.17$ cm^{-1}, $D = 6.0$ cm^{-1}.

involves the reciprocal of the effective g value, so for a given value of J, the splitting in gauss of the $g \sim 2$ nitroxyl signal is approximately three times the splitting in gauss for the $g \sim 6$ iron signal. Actually there are many transitions within the envelopes of the apparent doublets. As the strength of the interaction increases, the nitroxyl signal is spread over an increasingly large range of magnetic fields and becomes more difficult to detect. For $|J|$ > about 0.05 cm^{-1}, there are no signals that can be identified as "nitroxyl" peaks and the observed peaks occur at $g \sim 3$–10.

The EPR spectra of VIII–XI in frozen solution also exhibited peaks at $g = 2.7$ to about 10. Simulations of these spectra were obtained with $|J|$ between 0.12 and 0.17 cm^{-1} and values of r between 5 and 6 Å. Conformations with weaker spin–spin interaction were not observed for VIII–XI.

Temperature Dependence of EPR Spectra. The spectra of Fe(I)X, X = F^-, Cl^-, and OH^-, at 100 K are shown in Figure 2. The line widths in the spectra are broader than those observed at 6 K for Fe(I)Cl (Figure 1D) due to increased iron electron spin relaxation rates, but the positions of the peaks are unchanged. The spectra for Fe(I)X at 100 and ca. 5 K could be simulated with the same parameters except for line widths. $|J|$ was dependent on X^-, and values were in the range 0.07–0.17 cm^{-1}.

As demonstrated by the spectra in Figure 3, increasing the temperature had a much more dramatic effect on the spectra for the complexes with weaker electron–electron spin–spin interaction than for the complexes with $|J| > \sim 0.05$ cm^{-1}. At 7 K the spectrum of the nitroxyl signal for Fe(VII)Br showed a sharp signal superimposed upon a broadened signal due to a conformation with greater spin–spin interaction (Figure 3B). As the temperature was increased, the broad nitroxyl signal broadened further due to the increase in the iron electron spin relaxation rate. At 40 K the splitting of the nitroxyl signal by the iron was largely collapsed and the intensity of the signal that was broad at 7 K

(26) More, K. M.; Eaton, G. R.; Eaton, S. S. *Inorg. Chem.* **1985**, *24*, 3698.
(27) Fielding, L.; More, K. M.; Eaton, G. R.; Eaton, S. S. *J. Am. Chem. Soc.* **1986**, *108*, 8194.

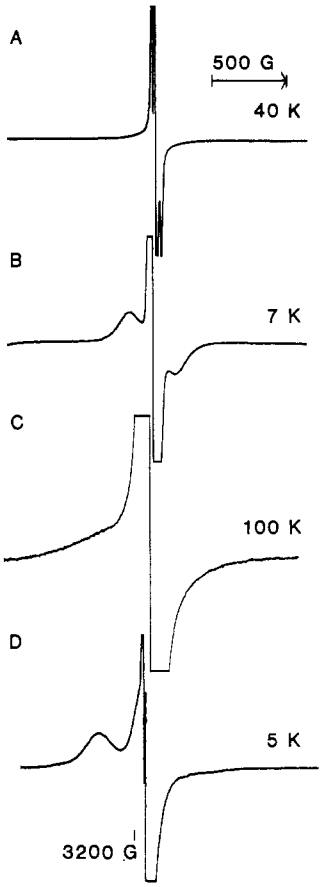

Figure 3. 2000-G scans of X-band (9.2 GHz) EPR spectra of the nitroxyl signals for spin-labeled iron porphyrins in frozen toluene solution: (A, B) Fe(VII)Br at 40 and 7 K, respectively; (C, D) Fe(II)Br at 100 and 5 K, respectively. The modulation amplitudes were 1–2 G for (A), (B), and (D) and 20 G for (C). The microwave powers were 2–4 mW for (A), (B), and (D) and 50 mW for (C).

was largely superimposed on the signal from the other conformation. Similarly, the broadened and shifted nitroxyl signal observed for Fe(II)Br at 5 K (Figure 3D) was severely broadened and partially collapsed at 100 K and was observed only at high signal amplification (Figure 3C). The collapse of iron–nitroxyl splitting with increasing temperature was reported previously for Fe(V)X.[27]

Since the iron electron spin relaxation rate at a particular temperature is proportional to zero-field splitting,[28] the relaxation rates for Fe(P)X are expected to increase in the order X = F^- < Cl^- < DMSO < Br^- (see values of ZFS in computer simulation section). Thus, the collapse of the nitroxyl splitting was more extensive at the same temperature for X = Br^- or DMSO than for X = F^- or Cl^-. For all of the complexes with $|J| < \sim 0.05$ cm^{-1} the iron–nitroxyl spin–spin splitting was partially resolved in the EPR spectra at 100 K for X = F^- or Cl^- but not for X = Br^- or DMSO. Thus, in general, observation of resolved electron–electron spin–spin coupling between high-spin iron(III) and nitroxyl radicals is likely to require spectra taken near 4 K unless the iron zero-field splitting is small.

Changing Populations of Conformations. The EPR spectrum of the iron $g_\perp$ signal for Fe(III)F in toluene solution at 100 K (Figure 4A) shows that a relatively small fraction of the molecules contribute to the signal at $g \sim 6$ that is due to conformations with weak spin–spin interaction. Much of the intensity is in the peaks at g values above and below 6 that are due to conformations with large enough spin–spin interaction to cause observable splitting of the iron signal. The integral of the sharp nitroxyl signal for Fe(III)F indicated that about 10% of the nitroxyl in the sample was in the weakly interacting conformation. Integration of the

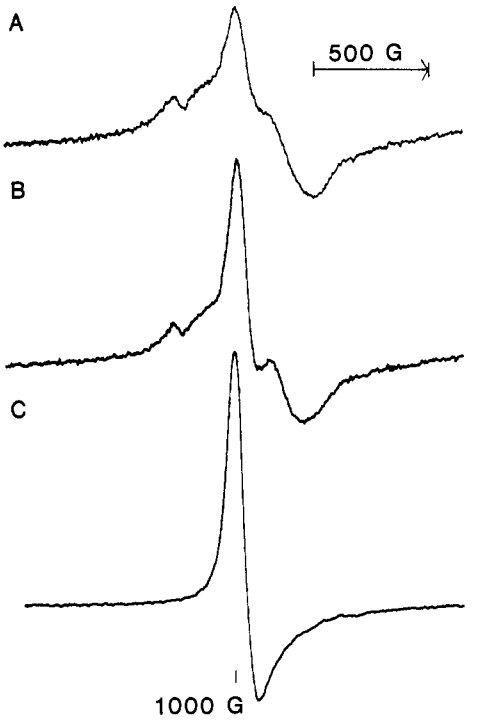

Figure 4. 2000-G scans of X-band (9.1 GHz) EPR spectra of the iron $g \sim 6$ signal for 1 mM Fe(III)F at 100 K: (A) in toluene solution; (B) in toluene containing 5 mM 1,3,5-trinitrobenzene; (C) in 2:1 chloroform:tetrahydrofuran solution.

sharp nitroxyl signals for 1 mM solutions of Fe(P)Cl, P = I–VII, indicated that the populations of the conformations with weak spin–spin interaction were between about 5 and 20%.

Although the spectra for Fe(P)X, P = III, V, and VII (Figure 1B–D) were dominated by the conformations with larger iron–nitroxyl interaction, the spectra for the corresponding Fe(P)-$(DMSO)_2^+$ complexes were dominated by conformations with sufficiently weak iron–nitroxyl interaction that the nitroxyl nitrogen hyperfine splitting was partially resolved. Integration of the sharp nitroxyl signal for Fe(I)$(DMSO)_2^+$ indicated that about 20% of the molecules were in the weakly interacting conformation. For Fe(P)$(DMSO)_2^+$, P = II–VII, the populations of the weakly interacting conformations were between 50 and 100%.

In 2:1 $CHCl_3$:THF solution the THF coordinates to Fe(P)X to give a six-coordinate complex.[29] In the EPR spectrum of Fe(III)F in 2:1 $CHCl_3$:THF solution (Figure 4C) most of the intensity of the iron $g_\perp$ signal was at $g \sim 6$, which indicated that most of the molecules were in the conformation with weak spin–spin interaction. In 2:1 $CHCl_3$:THF solution the populations of conformations with weak spin–spin interaction for Fe(P)X, P = I–VII, were similar to what was observed for the $(DMSO)_2$ adducts. The larger populations of the conformations with weak spin–spin interaction for Fe(P)$(DMSO)_2^+$ and Fe(P)(THF)X than for Fe(P)X show that coordination of a sixth ligand favored the conformations with weak spin–spin interaction.

Several conformations with differing magnitudes of spin–spin interaction have been observed previously for low-spin Fe(III),[7] Ag(II),[30] and Cu(II)[31] complexes of ortho-spin-labeled porphyrins. For the Ag(II) and Cu(II) complexes coordination of axial ligands resulted in conformations with weaker spin–spin interaction.[30,31] It was proposed that the conformations with stronger spin–spin interaction were due to weak interaction of orbitals from the ortho substituent with the porphyrin π orbitals or the metal orbitals.[30,31] When axial ligands were coordinated to the metal, either steric constraints or decreased donor/acceptor character of the me-

(28) LaMar, G. N.; Walker, F. A. *J. Am. Chem. Soc.* **1973**, *95*, 6950.

(29) Van Camp, H. L.; Scholes, C. P.; Mulks, C. F.; Caughey, W. S. *J. Am. Chem. Soc.* **1977**, *99*, 8283.

(30) More, K. M.; Eaton, G. R.; Eaton, S. S. *Inorg. Chem.* **1984**, *23*, 4084.

(31) More, K. M.; Sawant, B. M.; Eaton, G. R.; Eaton, S. S. *Inorg. Chem.* **1981**, *20*, 3354.

talloporphyrin made these weak orbital interactions less favorable. The impact of axial ligands on the conformations of the spin-labeled high-spin iron(III) complexes appears to be analogous to that which was observed for the Cu(II) and Ag(II) complexes.

1,3,5-Trinitrobenzene (TNB) forms a π complex with a pyrrole ring of FeTTPCl.[32,33] The spectrum of the iron signal for Fe(III)F in the presence of 5 equiv of TNB (Figure 4B) has a larger fraction of the intensity of the $g_\perp$ signal at $g \sim 6$ than was observed in toluene solution (Figure 4A). This indicates that complexation with TNB results in a larger population of the conformations with weaker spin-spin interaction. Complexation with TNB also favored the conformations with weaker spin-spin interaction for Fe(P)X, P = I, II, and IV-VII, X = F^- and Cl^-. Addition of TNB to the samples had little impact on the EPR spectra of VIII-XI or $Fe(P)(DMSO)_2^+$, P = I-VII.

Formation of π complexes with the porphyrin ring has been shown to influence the electronic structure of porphyrins.[34] For example, complexation of Fe(TPP)X with TNB decreases the affinity of the iron for axial ligands.[32] Also, interaction of one molecule of toluene with the porphyrin ring of $Mn(TPP)(H_2O)^+$ caused an increase in the length of the Mn-O bond to the coordinated water.[34] The decrease in the populations of conformations with stronger spin-spin interaction for Fe(P)X, P = I-VII, caused by formation of the TNB complexes again suggests that these conformations have weak orbital interactions between the ortho substituent and the porphyrin π orbitals or the metal orbitals.

NMR studies of Fe(TTP)X have shown that aggregation via π complexation between two porphyrin rings is significant in 5-30 mM solutions at -30 °C.[33] The concentration dependence of the EPR spectra of Fe(P)X between 0.1 and 10 mM was examined to check for effects of aggregation. The line widths in the spectra of VIII-XI increased as the concentration increased, but the spectra were otherwise unchanged. For Fe(P)X, P = I-VII, X = F^-, Cl^-, and Br^-, the line widths and the populations of the conformations with weaker spin-spin interaction increased as the concentration increased. It is proposed that the porphyrin-porphyrin π complexation influenced the conformational equilibria analogous to the effect of TNB complexation.

These spin-labeled iron porphyrin complexes have provided examples of iron-nitroxyl spin-spin interaction ranging from less than the line widths of the spectra to $|J| = 0.17$ cm^{-1}. This set of complexes has greatly expanded the range of demonstrated electron-electron spin-spin couplings in EPR spectra. The variety of conformations observed for these complexes precludes a correlation between molecular structure and the strength of the interaction. Complexes with rigid geometries are needed to provide those correlations.

Acknowledgment. The partial support of this work by NIH Grant GM21156 is gratefully acknowledged. Purchase of the IBM ER200 EPR spectrometer was funded in part by NSF Grant CHE8411282.

(32) Kabbani, A. T.; LaMar, G. N.; *J. Magn. Reson.* **1981**, *43*, 90.
(33) Snyder, R. V.; LaMar, G. N. *J. Am. Chem. Soc.* **1977**, *99*, 7178.
(34) Williamson, M. M.; Hill, C. *Inorg. Chem.* **1987**, *26*, 4155 and references therein.

Contribution from the Department of Chemistry, The University of North Carolina, Chapel Hill, North Carolina 27514, and United States Geological Survey, Reston, Virginia 22092

Synthesis and Spectral and Redox Properties of Three Triply Bridged Complexes of Ruthenium

Antoni Llobet,[1a,b] Maria E. Curry,[1a] Howard T. Evans,[1c] and Thomas J. Meyer*[,1a]

Received July 22, 1988

Syntheses are described for the ligand-bridged complexes $[(tpm)Ru^{III}(\mu\text{-}O)(\mu\text{-}L)_2Ru^{III}(tpm)]^{n+}$ (L = $O_2P(O)(OH)$, n = 0 (**1**); L = O_2CO, n = 0 (**2**); L = O_2CCH_3, n = 2 (**3**); tpm is the tridentate, facial ligand tris(1-pyrazolyl)methane. The X-ray crystal structure of $[(tpm)Ru(\mu\text{-}O)(\mu\text{-}O_2P(O)(OH))_2Ru(tpm)]\cdot 8H_2O$ was determined from three-dimensional X-ray counter data. The complex crystallizes in the trigonal space group $P3_221$ with three molecules in a cell of dimensions a = 18.759 (4) Å and c = 9.970 (6) Å. The structure was refined to a weighted R factor of 0.042 based on 1480 independent reflections with $I \geq 3\sigma(I)$. The structure reveals that the complex consists of two six-coordinate ruthenium atoms that are joined by a μ-oxo bridge (r_{Ru-O} = 1.87 Å; ∠RuORu = 124.6°) and two μ-hydrogen phosphato bridges (average r_{Ru-O} = 2.07 Å) which are capped by two tpm ligands. The results of cyclic voltammetric and coulometric experiments show that the complexes undergo both oxidative and reductive processes in solution. Upon reduction, the ligand-bridged structure is lost and the monomer $[(tpm)Ru(H_2O)_3]^{2+}$ appears quantitatively. All three complexes are diamagnetic in solution. The diamagnetism is a consequence of strong electronic coupling between the low-spin d^5 Ru(III) metal ions through the oxo bridge and the relatively small Ru-O-Ru angle.

Introduction

Of the μ-oxo complexes of ruthenium, the structurally characterized examples include (1) complexes such as $[(bpy)_2(L)Ru^{III}(O)Ru^{III}(L)(bpy)_2]^{4+}$ (L = H_2O, NO_2^-), in which there is a μ-oxo link between two Ru(III) sites,[2] (2) the triangular, planar structure in $[Ru_3O(L)_3(O_2CCH_3)_6]$ (L = H_2O, PPh_3), where the oxo group bridges three ruthenium ions, each pair of which is bridged by three acetate ligands,[3] and (3) ruthenium red $[Ru_3O_2(NH_3)_{14}]^{6+}$ and its analogues, which contain the oligomeric group N-Ru-O-Ru-O-Ru-N.[4]

From the results of previous studies, the μ-oxo link in compounds of Ru can sustain strong electronic coupling between the metal sites. The coupling can lead to significant modifications in the chemical and physical properties of the resulting materials

(1) (a) The University of North Carolina. (b) Fulbright "La Caixa" fellow, Barcelona, Spain. Permanent address: Departament de Química (Area 10), Universitat Autònoma de Barcelona, 08193 Bellaterra, Barcelona, Spain. (c) U.S. Geological Survey.
(2) (a) Phelps, D. W.; Kahn, E. M.; Hodgson, D. J. *Inorg. Chem.* **1975**, *14*, 2486. (b) Gilbert, J. A.; Eggleston, D. S.; Murphy, W. R.; Geselowitz, D. A.; Gersten, S. W.; Hodgson, D. J.; Meyer, T. J. *J. Am. Chem. Soc.* **1985**, *107*, 3855.
(3) (a) Cotton, F. A.; Norman, J. G. *Inorg. Chim. Acta* **1972**, *6*, 411. (b) Spencer, A.; Wilkinson, G. *J. Chem. Soc., Dalton Trans.* **1972**, 1570. (c) Cotton, F. A.; Norman, J. G.; Spencer, A.; Wilkinson, G. *J. Chem. Soc., Dalton Trans.* **1971**, 967.
(4) (a) Carrondo, M. A. A. F. d. C. T.; Griffith, W. P.; Hall, J. P.; Skapski, A. C. *Biochim. Biophys. Acta* **1980**, *627*, 332. (b) Smith, P. M.; Fealey, T.; Earley, J. A.; Silverton, J. V. *Inorg. Chem.* **1971**, *10*, 1943. (c) Geselowitz, D. A.; Wlodzimierz, K.; Meyer, T. J. *Inorg. Chem.* **1986**, *25*, 2015.

0020-1669/89/1328-3131$01.50/0